A Study of Interaction of Water and Model Compound of Poly(vinyl methyl ether)

Xiguo Zeng and Xiaozhen Yang*

State Key Laboratory of Polymer Physics and Chemistry, The Center for Molecular Science, Institute of Chemistry, Chinese Academy of Sciences, Beijing 100080, China

Received: July 2, 2004; In Final Form: September 10, 2004

Poly(vinyl methyl ether) (PVME) aqueous solution possessing specific bimodal phase diagram has been studied on the interaction of water and dimethyl ether (DME) as a model compound of PVME by using ab initio calculation (6-31+G*) and infrared spectroscopy. The most probable interaction configurations of DME with one to five water molecules were intensively searched in the present study. Among the configurations, we found two sorts of interactions appearing as specialties: the hydrogen bond (HB) and the quasi-hydrogen bond (QHB). We further studied the influence of the interactions on infrared band shifts for $\nu_s(CH_3)$ and ν(C−O) as a function of the number of water molecules in statistical average. Comparing with the experiments, the high concentration area and the low concentration area (with two different slopes) suffer from different interaction mechanisms. The former has HB and single-QHB, while the latter double-QHB and triple-QHB, besides the van der Waals and the electrostatic interaction. For understanding PVME hydration in details, we simulated the observation curve of the band shift versus the concentration by using adsorption procedures under three models. The result surprisingly indicates that water adsorption on PVME is not even distributed on each site of the monomer unit even though the polymer hydration is in the homogeneous phase.

1. Introduction

Poly(vinyl methyl ether) (PVME) is a water-soluble polymer that has the lower critical solution temperatures (LCSTs) with water at a moderate temperature around 35 °C and above that temperature the solutions separate into two phases.[1,2] Published information on properties of PVME, particularly its behavior in aqueous solutions, is summarized by Molyneux.[3] In 1997, Berghmans[4] found that the LCST-behavior of PVME is more complex than what can be expected from "classical" theoretical considerations and that the corresponding LCST-demixing curve is a bimodal shape with two minima that show a different molecular mass dependence. Such a behavior has attracted much attention on intermolecular interactions between water and the polymer.[5−8]

PVME having such a bimodal feature may result from the specific interaction of water and polymer. Usually, this interaction is twofold: the hydrophilic and the hydrophobic one. Consider the structure of PVME: it has hydrophilic sites (ether oxygen) that can be hydrogen bonded with the neighboring water molecules.[9] Hydrogen bond (HB) is an immemorial subject in science; as mentioned by Scheiner,[10] the HB must contain the proton donor with the pertinent hydrogen covalently bonded to an electronegative atom and an acceptor molecule including an electronegative atom with at least one lone pair of electrons. As the two molecules approach, the hydrogen atom forms a sort of "bridge" between them. The lone pair of the acceptor atom is pulled toward the bridging proton to form a weak bond. To the complex of PVME and water, the water molecule is the proton donor, while the ether oxygen on PVME is the acceptor. Since there are only two lone pairs of electrons on ether oxygen, it can certainly form two HBs with two water molecules.

In addition, there are also hydrophobic groups, particularly methyl groups, on PVME. They can destabilize the solution by altering the normal water structure near the chains, which have been interpreted by the "icebergs" concept of Nemethy and Scheraga[11] and Frank and Evans.[12] The iceberg is a description of water interacting with the hydrophobic groups. It represents a microscopic region, in which water molecules are tied together in some sort of quasi-solid structure, and not exactly icelike.

The above two sorts of interactions have been extensively studied in many polymer systems.[13−15] For PVME, near-infrared, viscometric, calorimetric measurements,[9] and so forth were used in study of its aqueous solutions. On the basis of observed three regions distinguished by the characteristic temperature, the endothermic heat of phase separation, and the spectral band shift, it was presumed[9] that water molecules in the system could be classified into three kinds: an average of 2.7 water molecules on each repeat unit as a cooperative polymer−water complex through HB to the ether oxygen, a second average of 2.3 additional water molecules forming a cluster around the hydrophobic sites of each repeat unit as the iceberg structure, and the rest of the water beyond 5 molecules per repeat unit being free in the system. Even this model looks reasonable in description of the interactions; up to now, there has been no evidence in terms of microscopic structures to support it.

A recent study[16] has found that hydration and dehydration of PVME can be monitored by infrared band shifts of C−O stretching mode and C−H stretching mode of methyl group. The former relates to interaction with water on a hydrophilic group and the latter on a hydrophobic group. The author plotted[16] the infrared band frequencies of the two modes versus the concentration of PVME and found a bending point at ∼40 wt % and also two slopes: one is small in the low concentration side and the other large in the high concentration side. This result is almost the same with the FTIR data we obtained as plotted in Figure 1. The author concluded that in the small slope area the methyl and ether groups are fully hydrated, and in the

* To whom correspondence should be addressed. Fax: +86-10-62571123; e-mail: yangx@iccas.ac.cn.

10.1021/jp047076s CCC: $27.50
Published on Web 10/20/2004

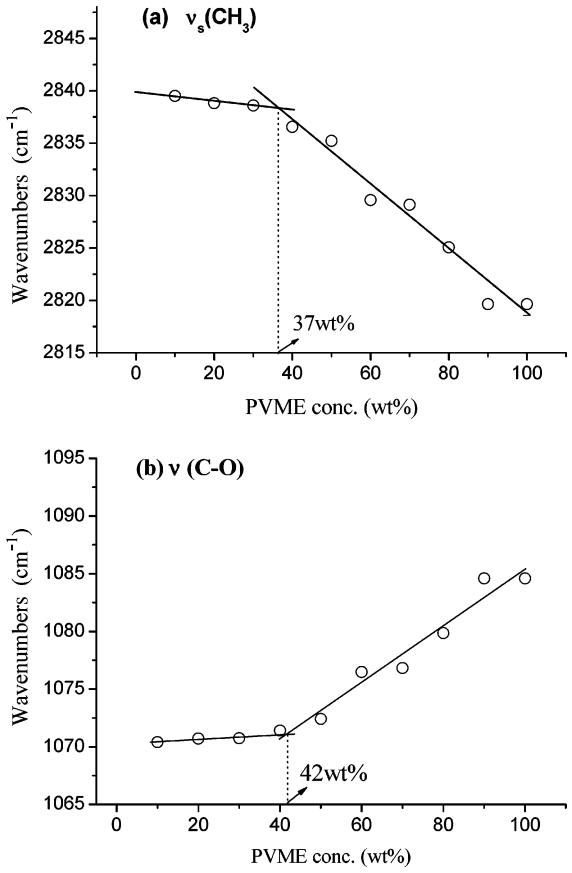

Figure 1. (a) Positions of the $\nu_s(CH_3)$ band and (b) positions of ν(C−O) band of PVME measured in H_2O are plotted against polymer concentration.

large slope area these groups may be partly dehydrated. Obviously, a further study is needed to gain insight into the interaction at the molecular level. In the large slope area, we should learn how a small amount of water adsorbs on the polymer by HB. In the small slope area, the above description that all the groups on the polymer are fully hydrated seems a discrepancy. This is because that the interaction between the polymer and water fully works or keeps no change, but the observation shows the frequency shift still occurred and made a small slope there. It indicates there must be a change in the interaction between water and the polymer in that area. Evidently, we have to find out this interaction in the system, and it is necessary to study various interaction configurations between PVME and water and the corresponding frequency shifts in infrared of vibration modes involved in detail.

In the present study, in addition to measured infrared spectral bands for various concentrations of PVME in water, a model compound, dimethyl ether (DME), has been used to study the detail interaction of water and PVME by ab initio calculation. The reason for use of DME is that the C−O stretching mode and C−H stretching mode on the side chain of PVME are of the group frequency, more localized modes, and insensitive to the conformation of polymer backbone. This study aimed for a better understanding of what interaction differences among the possible configurations exist, how the interactions affect the IR spectra band behavior of the polymer, and what the polymer hydration details are. An examination took place on interaction of DME with one to five water molecules, which results in a large number of interaction configurations. Infrared band shifts of $\nu_s(CH_3)$ and ν(C−O) of the compound influenced by the interactions were calculated through a statistical average of the obtained configurations. We found that in the large slope area the band shift is predominately caused by HB and in the small slope area by the interaction of the quasi-hydrogen bond (QHB) on the rest sites of the methyl groups. According to obtained band shift as a function of the number of water molecules, we built several adsorption models to simulate the observation curve of the band shift versus the concentration. The result obtained delivers a message that the adsorption distribution of water on PVME is not even along the chain.

2. Experiments and Calculations

PVME was obtained from Aldrich. The molecular weight of the polymer, determined by gel permeation chromatography, was $M_w = 20$ kg/mol. The PVME solution was prepared by incubating the polymer in deionized water for several days at room temperature to equilibrium. Concentrations are given in weight of the polymer.

All spectra were recorded on a Bruker EQUINOX 55 spectrometer and processed by the Bruker OPUS program. A sample solution was put between two calcium fluoride (CaF_2) windows without spacers and the sample thinness was adjusted to make the maximum absorbance of target IR bands to smaller than 2 absorbance units. The background spectrum for one cycle of the measurement was obtained with a clear CaF_2 window. The spectra were obtained by averaging 32 scans at a 2 cm^{-1} resolution. A Bruker P/N 21525 series variable temperature cell was used.

In addition, as mentioned in the earlier study,[9] it was found that five water molecules interact with PVME in each repeat unit. Therefore, several configurations of the model compound interacting with zero to five water molecules were designed and calculated in the Gaussian 03 sets programs[17] with MP2 method and the 6-31+G* basis set, which has been widely used in the calculation of water clusters.[18−23] After the energy minimization of the most probable configurations, we calculated the vibrational frequencies of each complex. Furthermore, the band shape function was built up by using a mixture of Lorentzian and Gaussian functions[24] in a ratio of 9:1, and the bandwidth was fixed at 8 cm^{-1}.

The statistical weight factor σ_k for each configuration was obtained by Boltzmann distribution (eq 1), and the partition function Z and the probability P_k for each configuration were obtained by using eqs 2 and 3. The simulated IR spectrum $I(\nu)$ for one of the DME/water systems was then calculated by using eq 4, where ΔE_k is the energy difference between the energy in kth configuration and the lowest energy which is set for the zero point. Here, RT is simply taken as 600.

$$\sigma_k = e^{-\Delta E_k/RT} \tag{1}$$

$$Z = \sum_{k=1}^{m} e^{-\Delta E_k/RT} \tag{2}$$

$$P_k = \sigma_k/Z \tag{3}$$

$$I(\nu) = \sum_{k=1}^{m} I_k(\nu)\cdot P_k \tag{4}$$

3. Results and Discussion

3.1. DME as the Model Compound of PVME. In the present study, we used dimethyl ether (DME) as the model compound of PVME, and one of the methyl groups is deuterated. The reason for the choice is fourfold.

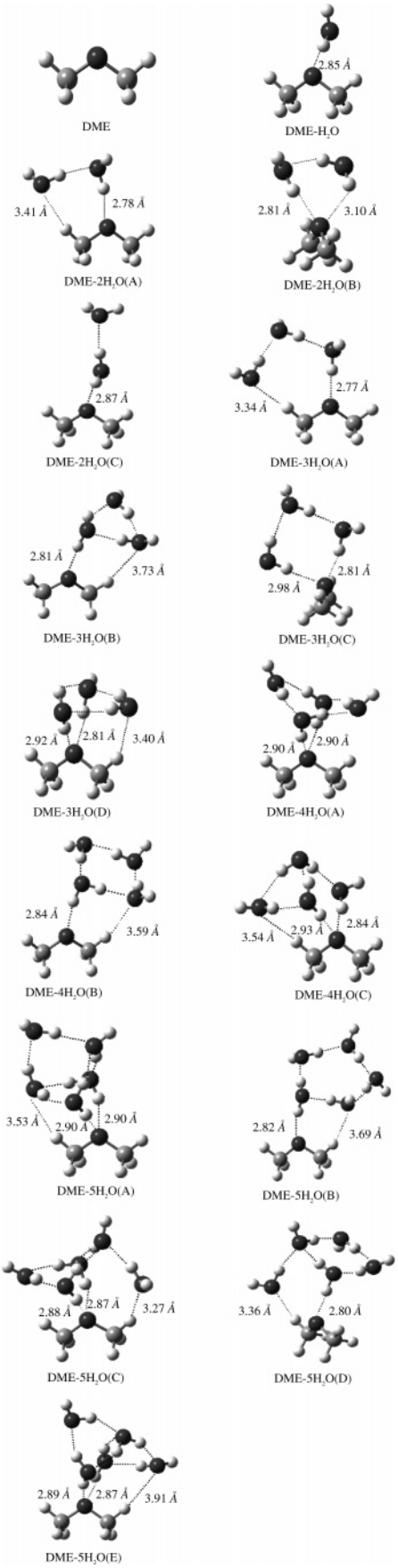

Figure 2. Geometry of the optimized configurations of DME·nH$_2$O ($n = 0\sim5$).

First, DME has the consistent chemical structure with the side chain of PVME. Second, the vibration modes interested in the present study are very localized. They are the C−H stretching mode of methyl and the C−O stretching mode, and both appear in the range of so-called "group frequency". Since the localization, DME has the same spectral behavior with that of PVME, that is, the blue shifts of $\nu_s(CH_3)$ band and the red shift of ν(C−O) band take place when interacting with water, as observed by Engdahl.[25]

Third, the two modes, $\nu_s(CH_3)$ and ν(C−O), used here are not greatly influenced by the conformation of main chain backbone. The methyl is at the end of the side chain and almost free from the conformation. The ether oxygen −O− is also in the side chain and interacts with neighbor atoms in different conformations through ven der Waals interaction, which is one magnitude smaller than HB interaction. Additionally, as the system studied here is under a constant temperature, conformation of PVME will not change significantly. The frequency of the modes is thus hardly affected by the conformation.

Finally, the DME here with a normal methyl and a deuterated methyl is to remove coupling between the two methyl groups, especially in the C−H stretching mode. Then, the model compound possesses more close nature to PVME through the specified window.

TABLE 1: Energy (kcal/mol) for the Optimized Configurations of DME·nH$_2$O[a]

	A	B	C	D	E
DME·2H$_2$O	0	2.17	4.40		
DME·3H$_2$O	0	0.26	1.21	2.38	
DME·4H$_2$O	0	1.65	4.57		
DME·5H$_2$O	0	0.79	0.85	2.53	4.49

[a] Results were computed with the MP2 method and 6-31+G* basis set.

3.2. The Configurations of Interaction between Several Water Molecules and DME. As mentioned in the earlier study,[9] it was presumed that in each repeat unit five water molecules interact with PVME. In the following sections, we reported a systemic investigation on the interactions of DME with nH$_2$O ($n = 1\sim5$).

A critical point in the present study is to find the most probable configuration structures of DME·nH$_2$O ($n = 1\sim5$), which are bases of investigation on the interaction. In recent years, water clusters $(H_2O)_n$ have been studied extensively both experimentally[26,27] and theoretically.[28−33] When $n = 2\sim6$, there are a huge number of possible configurations. The significant configurations of water clusters have been figured out by quantum mechanics. On the basis of these structures, we put the DME molecule into the optimal water clusters to take the place of one proton acceptor water molecule, and then a series of structures of DME·nH$_2$O ($n = 2\sim5$) complexes were calculated. Figure 2 shows the optimal structures of DME with zero to five water molecules. Those structures with energy more than 5 kcal/mol higher than the global minimum of each system have been abandoned. To distinguish various configurations in a complex system, we label A, B, C, ... in an order with an increase of energy appending the species DME·nH$_2$O as shown in Figure 2. The relative energies of these structures are listed in Table 1, where the energy of the most stable structure in each system is set to be zero.

From these optimal structures, we found that there are two evident characteristics. First, two sorts of interactions between water and DME, specifically the hydrophilic interaction on ether oxygen and the hydrophobic interaction on methyl group, coexist in many configurations, especially in those with less water or in the high concentration of PVME, such as DME·2H$_2$O(A) and DME·3H$_2$O(A) (Figure 2). This therefore indicates that in

TABLE 2: The Interaction Energy (kcal/mol) of HB and QHB Interaction[a]

1st HB	HB (in water dimmer)	2nd HB	QHB
7.76	6.24	1.64	2.31

[a] Results were computed with the MP2 method and 6-31+G* basis set.

the high concentration of PVME, the hydrophobic interaction of water and methyl group also exist. Second, in less water, when $n \leq 3$, the ether oxygen prefers forming only one HB with water to double HB, even though the ether oxygen is able to accept two HBs. However, when $n \geq 4$, such a tendency is inversed, and we found that formation of two HBs on the ether oxygen turns to be more stable than that of only one HB.

3.3. Two Sorts of Interaction Mechanism between PVME and Water. *3.3.1. Character of Interaction between DME and Water.* In PVME aqueous solution, water molecules interact with a hydrophilic group, the ether oxygen, and a hydrophobic group, the methyl. Such interaction cases can be modeled by DME interacting with water. As is well known, the former interaction results in the HB, and the latter the van der Waals (vdW) interaction and the electrostatic interaction as well defined in the force field of classical mechanics.[34] Additionally, we found in the present study that a distinct sort of interaction between the methyl and water exists in the system, such as in the configuration of DME·2H_2O(A). This interaction was recognized as a weak HB through C−H···O by Scheiner.[35] In his study, this weak HB is between water and methane, but in our case, it is between the water and the methyl group. For convenience, we simply call it "QHB" (quasi-hydrogen bond) as mentioned above.

3.3.1.1. Hydrogen-Bonding Cooperativity. For the model of DME·H_2O, there is a deep potential well located at the ether oxygen of DME; therefore, wherever the water molecule was put at the beginning, it always migrated and bonded with the ether oxygen instead of the methyl group after energy minimization by either quantum mechanics with Gaussian03 (MP2/6-31+G*) or molecular mechanics (MM) under Dreidingforce field (see Figure 2). The distance between ether oxygen and its bonded water R(O···O) is 2.84 Å, a little shorter than R(O···O) of water dimmer.[35] As shown in Table 2, obtained interaction energy of the HB between water and ether oxygen of DME is about 7.76 kcal/mol, larger than HB energy of 6.24 kcal/mol in water dimmer. It shows that the strength of HB between water and −O− group is larger than that between water, which is consistent with homologous spectroscopic observations.[36]

Since each ether oxygen has two lone pairs of electrons, it is regarded to be able to act as the double-proton acceptor forming two HBs. Recently, many scientists studied cooperative phenomena of HB.[37−40] They found that the molecules prefer to be one donor and one acceptor, thus becoming cycles or chains. On the formation of HB, the electron density removes from an acceptor, which is turned to be a poorer proton acceptor. The acceptor therefore is less inclined to accept a second HB. This is called "negative cooperativity".[41] The same phenomena occurred in our present study. As shown in Table 2, the energy of the second HB was around 1.64 kcal/mol, much less than the traditional HB energy, which is due to the "negative cooperativity" of the first HB.[41] It is also much less than that of the HB between water, which leads that water molecules prefer to bond to one another than to form a second HB with the same ether oxygen. Correspondingly, bond length of the second HB increases to more than 2.90 Å. Such as in the case of DME·2H_2O(B), the first HB is 2.81 Å and the second 3.10 Å. Also, 2.81 Å and 2.98 Å is for DME·3H_2O(C), 2.81 Å and 2.92 Å for DME·3H_2O(D).

In the present study, we found that the negative cooperativity is not only in the asymmetric pair of HB to the ether oxygen as mentioned in the above cases, but also in the symmetric pair of HB; there, such as in DME·4H_2O(A), the first HB has the same length, 2.90 Å, as that of the second HB. The same peculiarity occurs in DME·5H_2O(A), DME·5H_2O(C), and DME·5H_2O(E). In these cases, the two HBs have symmetric bond lengths. The reason of having such symmetric hydrogen-bonding structure is that the two hydrogen-bonded water molecules have the same bonding behavior, that is, they both act as double donor and single acceptor; thus, the two HBs from the similar water share the same ether oxygen becoming the same category. Therefore, even though the first HB is in a strong strength, if there forms a second HB, which has a chance to gain some electron densities from the first one and to shrink its own bond length to around 2.90 Å, the first HB extends its length to the same value. It manifests that the symmetrization makes the distinct two HBs become two symmetric ones with a midstrength between the strong HB (in length of 2.81 Å) and the weak HB (3.10 Å). They are defined here as the two symmetrized HBs. Accordingly, the interaction energy of one of the symmetrized HBs thus increases beyond that of the second HB. Since this symmetrized HB needs the symmetrized interaction structures, the symmetrization merely occurs for DME·$n$$H_2O$ with $n \geq 4$, observed in the present study.

3.3.1.2. Quasi-Hydrogen Bond. QHB has been studied by Scheiner[35] in the interaction between water and methane. It is proved that the C−H···O interaction is a weak HB, or QHB, here. In the present study, we found that QHB appears in several configurations, such as DME·2H_2O(A), DME·3H_2O(A), DME·3H_2O(D), DME·4H_2O(B), and so forth. In these complexes, QHB has an angle of the C−H···O between methyl and water larger than 150°,[42] namely, around 180°. The average value of energy collected in the calculation for QHB is about 2.31 kcal/mol as shown in Table 2. This energy is larger than that of the C−H···O interaction of CH_4/H_2O,[35] which is reasonable because the polarity of the proton donor is increased, which makes the corresponding increment of the interaction energy. The same mechanism happens in replacing the H atom of CH_4 by a F or Cl atom as reported by Scheiner and Hobza.[35,43] Equilibrium intermolecular separations of QHB in the complexes were studied. Averagely, in the present QHB between DME and water the R(C···O) distance lies in the 3.4∼3.6 Å range, a little shorter than 3.6∼3.7 Å for H_3CH···OH_2.[35]

3.3.2. Spectral Influence of the Interactions. 3.3.2.1. Influence of HB on Both ν(C−O) and $\nu_s(CH_3)$. Experimentally, the ν(C−O) band of PVME shifts to lower wavenumbers when hydration occurs to the system, and meanwhile the $\nu_s(CH_3)$ band undergoes a blue shift as shown in Figure 1. It is understandable that the band shifts are caused by the CH_3−O− group of PVME forming HB with water and thus inducing changes in electronic structure of the group. As listed in the left part of Table 3, on formation of HB, net charges of H atoms of the methyl group become more positive, while that for the C and O atoms acquire more negative. This electronic change leads to C−H bond length shortening (the right part of Table 3) and corresponding vibration frequency shifting up in our calculation as mentioned below. This phenomenon was experimentally validated by using a matrix isolation method in argon. Engdahl et al. observed a blue shift of $\nu_s(CH_3)$ band of DME when an HB formed between ether oxygen and water.[25] It was rationalized that there exists

TABLE 3: The Changes of Atomic Charges (millielectrons) and Bond Length (Å) of DME on Effect of Specified HB Interactions[a]

	Δe						Δr				
	C[b]	O	C[c]	H[d]	H	H	C[b]−O	C[c]−O	C[c]−H[d]	C[c]−H	C[c]−H
1st HB	−4	−82	−4	9	11	16	0.008	0.008	0	−0.002	−0.002
2nd HB	−14	−28	−13	28	6	0	0.001	0.007	−0.001	−0.001	0
sym-H B	−15	−63	−11	9	9	9	0.008	0.006	0	−0.001	−0.001
QHB	11	−23	−36	88	−8	−15	−0.003	0.007	−0.002	0	0

[a] Results were computed with the MP2 method and 6-31+G* basis set. [b] C is in the deuterated methyl group. [c] C interacts with water directly by QHB. [d] H interacts with water directly by QHB.

the hyperconjugation between O and methyl of DME: electron density from the lone pairs on the oxygen atom are donated to π^* orbitals on the methyl groups[44] therefore causing the C−H bonds to be weakened. When HB happens to the oxygen, the oxygen lone pair electron density will decrease, which leads to a decrease in the extent of the hyperconjugation and thus to a strengthening and shortening of the C−H bonds and the blue shifting of the $\nu_s(CH_3)$ band.[45] At the same time, lone pair electrons on the ether oxygen atom are withdrawn by hydrogen of water upon the formation of HB; therefore, the electron density of C−O bond is reduced, and thus the red shift of the ν(C−O) band takes place.

As mentioned above, HB appears in two categories: the single HB (the stronger) and the second HB (the weaker). The two having different effects on spectral frequency was found in the present study. Since the shrinkage of C−O bond and the stretch of C−H bond both take place in HB formation, the calculated frequency of ν(C−O) band shifts down 12 cm^{-1}, and the indirect effect of HB on $\nu_s(CH_3)$ mode is about a blue shift of 16 cm^{-1}. The same results were obtained by Barnes et al.[45] For the second HB, when it links on the same ether oxygen, the effect on frequency of the two modes was obtained from a contrast of the frequency of DME·2H$_2$O(B) and that of DME·H$_2$O. Such an estimation giving the effect of the second HB is that ν(C−O) has a red shift of 9 cm^{-1} and $\nu_s(CH_3)$ a blue shift of 3 cm^{-1}. It is interesting that the second HB is able to make more than a half shift than that of the first HB for ν(C−O) mode and a less than half shift for $\nu_s(CH_3)$ mode.

3.3.2.2. Influence of QHB on the Vibration Modes. As mentioned by Scheiner,[35] QHB between water and CH_4 will also lead to blue shift of C−H stretching band. But to the PVME aqueous solution, how the QHB between water and methyl group affects the spectral band shift is usually not well realized. Here, we discussed the induction effect on ν(C−O) band and the direct effect on $\nu_s(CH_3)$ band from QHB.

Generally, the effect can be obtained by a contrast of frequency between a configuration with QHB and a configuration without QHB, such as the one of DME·2H$_2$O(A) and the one of DME·H$_2$O in Figure 2. Actually, to extract the influence of QHB on the vibration modes is difficult. This is because one cannot make a configuration with only interaction of QHB; usually, it must have an HB like in the above two configurations. Additionally, as the cooperativity between water, one hardly finds the same strength of HB in different configurations. For instance, the above two configurations do not have the same HB since they have different HB lengths (2.78 Å and 2.85 Å). We examined all the configurations with one HB and one QHB, and the calculations are listed in Table 4. The first row in Table 4 is for the configuration without QHB and the other ones are with QHB. The difference of the data between the first row and the other rows is considered as the contribution of QHB to the vibration modes. The contribution lies in a range. Since the configuration of DME·4H$_2$O(B) has a quite similar HB with a length of 2.84 Å as the standard HB (2.85 Å) of DME·H$_2$O, contribution of the configuration can be accepted as an average for QHB. As a result, QHB contributes ∼4 cm^{-1} blue shift to the ν(C−O) mode and ∼5 cm^{-1} red shift to the $\nu_s(CH_3)$ mode. This indicates that the influence of QHB is opposite to that of HB for the two vibration modes.

TABLE 4: The Effect of QHB on Frequencies (cm^{-1}) of the Vibration Modes[a]

models	ν(C−O)	$\nu_s(CH_3)$	$\nu_{as}(CH_3)$	
DME·H$_2$O (without QHB)	1187.4	3085.7	3162.6	3237.1
DME·nH$_2$O (with QHB)				
DME·2H$_2$O(A)	1188.9	3084.4	3161.9	3247.4
$\Delta\nu$	1.5	−1.3	−0.7	10.3
DME·3H$_2$O(A)	1188.4	3081.4	3157.7	3255.6
$\Delta\nu$	1.0	−4.3	−4.9	18.5
DME·3H$_2$O(B)	1192.3	3082.1	3157.5	3238.4
$\Delta\nu$	4.9	−3.6	−5.1	1.3
DME·4H$_2$O(B)	**1191.1**	**3081.2**	**3156.3**	**3241.7**
$\Delta\nu$	**3.7**	**−4.5**	**−6.3**	**4.6**
DME·5H$_2$O(B)	1192.7	3080.9	3155.6	3239.3
$\Delta\nu$	5.3	−4.8	−7	2.2
DME·5H$_2$O(D)	1186.8	3078.4	3154.7	3254.1
$\Delta\nu$	−0.6	−7.3	−7.9	17

[a] Results were computed with the MP2 method and 6-31+G* basis set.

It seems a discrepancy of the result for C−H stretching mode compared with Scheiner's calculation.[35] He pointed out that QHB makes C−H stretching have a blue shift. It is not like a red shift of C−H stretching for methyl as calculated here. Detailed results show us that the two calculations have the same conclusion. For clearness, we sort the complicated problem into several points. (1) The Scheiner interaction of methane with water leads to four stretching modes for C−H, a symmetry stretching mode and three asymmetry modes. He found that one of the asymmetry modes has a blue shift and that this mode with the highest frequency is mainly contributed from the very C−H which forms the QHB. (2) In our case, there are three stretching modes for C−H, a symmetry mode and two asymmetry modes, and the highest stretching mode (asymmetric) also has a blue shift of 4.6 cm^{-1}, and the other modes have a small red shift (in the row with bold font of Table 4). (3) Our result for various modes is consistent with Scheiner's. (4) However, the experimentally interesting vibration mode is the symmetric stretching mode of methyl, $\nu_s(CH_3)$,[16] which has never been studied with QHB interaction before. This vibration mode is the focus in the present study.

The effect discussed above is only related to the QHB with just one H atom in the methyl bonding to the O atom of water. This is called "single-QHB". When water increases in the system, the other C−H bonds on the same methyl may also have chances to interact with water by QHB. They are then named "double-QHB" and "triple-QHB". In the present study, we examined these QHB effects on the vibration modes. With a few molecules, it is difficult to simulate the bulk water

environment. However, we did approximate models in handling the problem. According to the result of single-QHB effect on the individual C−H bond, the C−H bond forming QHB must shorten 0.002 Å (see Table 3); we in turn set the other C−H bonds the same length, and thus have two models for the double-QHB and the triple-QHB. Calculated results show that double-QHB makes the direction of frequency shift change, namely, a very small blue shift of $\nu_s(CH_3)$ takes place when effected by the double-QHB. Furthermore, considerable blue shift of this mode can be obtained under the effect of the triple-QHB. This manifests that experimentally in the water-enhanced system the increase of the double-QHB and the triple-QHB stabilizes the system and makes the small slope of the frequency shift. The calculation also confirmed the similar behavior of the double-QHB and the triple-QHB for ν(C−O) mode and is consistent with experiments.

3.3.3. Different Interaction Mechanisms. From the influence on the spectral band shift of the two sorts of interactions, one may obtain a better understanding of why there exists bending points on the band shift curves of $\nu_s(CH_3)$ and ν(C−O) mode (Figure 1). It is clear that the bending points are caused by different interaction mechanisms of water and PVME. In the high concentration range, corresponding to the large slope area, all the efficient interaction, HB, second HB, and single-QHB work simultaneously. Even though the single-QHB will cause a small red shift of $\nu_s(CH_3)$ band and a blue shift of ν(C−O) band, the opposite shifts caused by HB of the two bands are much larger and stronger. As a result, a large blue shift of $\nu_s(CH_3)$ and red shift of ν(C−O) is usually obtained in the experimental observation. As water increases, when concentration of the PVME reaches the range below 40 wt %, ether oxygen atoms on PVME have been fully hydrated with double-HB, and one of the C−H bonds in all methyl groups has also bound with water by single-QHB; consequently, there is no chance to form more HB or single-QHB in the system. In such a situation, late joined water molecules have a chance to form the double-QHB and the triple-QHB on methyl groups. As the enhancement of water, the methyl groups gradually become fully hydrated with multiple-QHB. Therefore, in the low concentration area, the main factor causing further shift of spectral bands is multiple-QHB. As calculated above, such fully interacted methyl undergoes a gentle blue shift of $\nu_s(CH_3)$ stretching mode, which is consistent with a small slope found in experiment.

3.4. Hydration Feature of PVME in High Concentrations. *3.4.1. Spectral Band Shift as a Function of the Number of Water Molecules.* We have calculated the band frequency of $\nu_s(CH_3)$ and ν(C−O) of each configuration in Figure 2, and on the basis of the energy differences, their probabilities have also been calculated. The results are listed in Table 5. These frequencies are not merely from vibration modes but from superposition of concerned modes with their intensities using a band shape function (Lorentzian and Gaussian Function) as mentioned in section 2. Furthermore, statistical averaged IR spectra for each DME·nH$_2$O (n = 0∼5) system can be obtained by using the four equations also shown in section 2. These simulated average IR spectra in two ranges of the $\nu_s(CH_3)$ mode and ν(C−O) mode for DME·nH$_2$O (n = 0∼5) are shown in Figure 3, and peak positions of them are listed in Table 5. One may find that the frequencies of the two modes in Table 5 are systematically smaller than that in Table 4. This is because the former data are adjusted by a correct factor, which is usually used in ab initio calculation. In the present study, this factor is 0.94, which is obtained from comparison of statistical averaged DME spectra and the observed PVME spectra. On a whole, the last two

TABLE 5: The Frequencies (cm^{-1}) of the Two Modes for All Configurations[a]

			individual data		statistical average	
		probability	$\nu_S(CH_3)$	ν(C−O)	$\nu_S(CH_3)$	ν(C−O)
DME			2820	1105	2820	1105
DME·H$_2$O			2836	1093	2836	1093
DME·2H$_2$O	A	0.9883	2835	1095	2835	1095
	B	0.0110	2839	1084		
	C	0.0006	2834	1095		
DME·3H$_2$O	A	0.5554	2835	1093	2835	1095
	B	0.3601	2834	1098		
	C	0.0739	2846	1084		
	D	0.0105	2843	1082		
DME·4H$_2$O	A	0.9395	2842	1080	2842	1084
	B	0.0601	2833	1097		
	C	0.0005	2847	1082		
DME·5H$_2$O	A	0.6554	2846	1084	2844	1084
	B	0.1757	2833	1098		
	C	0.1589	2839	1077		
	D	0.0097	2830	1093		
	E	0.0004	2846	1084		

[a] Results were computed with the MP2 method and 6-31+G* basis set.

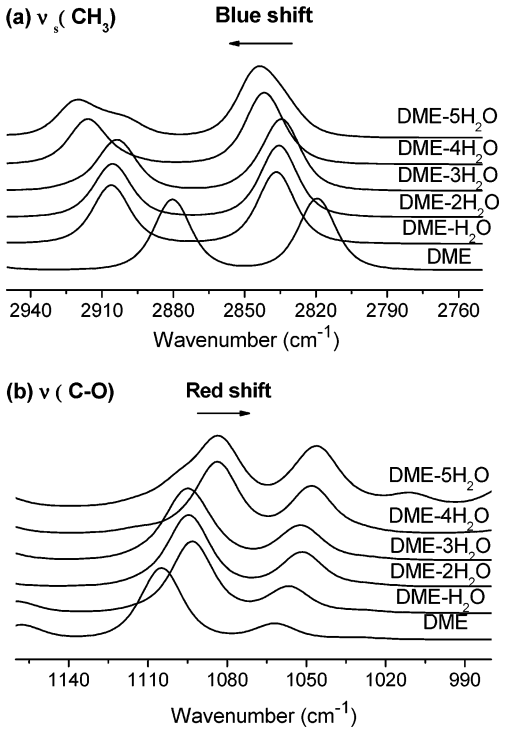

Figure 3. The simulated IR spectra of C−H stretching band (a) and C−O stretching band (b). Arrows in figure indicate increase or decrease in wavenumbers as the number of water molecules increase.

columns in the table show that as the number of water molecules increases, $\nu_s(CH_3)$ has a blue shift, while ν(C−O) has a red shift. Averaged band shifts of $\nu_s(CH_3)$ and ν(C−O) mode caused by different numbers of water molecules are shown in Table 6. With an increase of the number of water molecules, the shift of the two modes goes downward a little and then increases to the maximum. The configuration with two water molecules has a 15 cm^{-1} shift for $\nu_s(CH_3)$ and a 10 cm^{-1} shift for ν(C−O). These values are smaller than that of the one with one water molecule. This is because that as mentioned in section 3.3.2, HB gives large band shifts for both the modes while the single-QHB gives a smaller band shift in the opposite direction. This contrast causes a decrease in the shifts. When the number of

TABLE 6: The Band Shifts (cm^{-1}) Caused by Different Numbers of Water Molecules[a]

	$\Delta\nu_S(CH_3)$	Φ_n	$\Delta\nu(C-O)$	Φ_n
DME·H_2O	16	0.667	−12	0.571
DME·$2H_2O$	15	0.625	−10	0.476
DME·$3H_2O$	15	0.625	−10	0.476
DME·$4H_2O$	22	0.917	−21	1.000
DME·$5H_2O$	24	1.000	−21	1.000

[a] Results were computed with the MP2 method and 6-31+G* basis set. Φ_n is the normalized fractions of the configuration with n water molecules for the two modes.

water molecules is beyond 3, the second HB comes in and further increases the band shift to the maximum.

3.4.2. Simulation Details of Hydration Process. Since we calculated the most probable configurations of DME with different numbers of water molecules and simulated corresponding spectra for the vibration modes as observed in experiments, we certainly have the chance to simulate the hydration process by using both statistical averaged band shifts of interaction with various numbers of water and an adsorption procedure of water on PVME, specially in the higher concentration area, from 100 wt % to ~40 wt %, or in the high slope range.

Considering a PVME chain with 100 repeat units that is used here, then the number of water N_W runs from 0 to 500. When $N_w = 500$, each repeat unit of the polymer has five water molecules in average, the hydration process reaches the bending point. Calculated band shifts of DME for the two modes are listed in Table 6. As the calculation using model compound DME is not with real PVME, the band shifts to the bending point observed as 17 cm^{-1} and 13 cm^{-1} for $\nu_s(CH_3)$ and $\nu(C-O)$ mode, respectively, are different values from the calculations (24 cm^{-1} and 21 cm^{-1}). We have to use a parameter, Φ_n, to connect the two resources. It is a fraction of normalized band shift, which is normalized from the calculated data in Table 6. The subscript n here is for the nth adsorption state or the adsorption state with n water molecules ($n = 0\sim5$). By using this factor to simulate the observed spectral shift, we then obtain a corrected band shift for nth adsorption state:

$$\Delta\nu_n = \Delta\nu_{max}\cdot\Phi_n \tag{5}$$

where $\Delta\nu_{max}$ is obtained from experimental spectra, which is the maximum band shift observed for the hydration at 40 wt % of PVME relating to the initial frequency of the pure PVME.

During the hydration process, each side group of PVME adsorbs water in several ways. Statistically speaking, there are six adsorption states in the present study: the empty state (with zero water), the first state (with one water), the second state (with two waters), ... the nth state (with n waters, $n = 0\sim5$). The adsorption state consists of several interaction configurations, which are in the same category (Figure 2). Property of the adsorption state comes from a combination of the interaction configurations, which are weighted by Boltzmann factors. The fraction of nth adsorption states f_n is a ratio of the number of the nth state versus the 100 repeats. In an adsorption procedure, one can calculates f_n at any step of the run. Taking all the adsorption states into account, one is able to simulate the band shift ν close to the observations, if the procedure is nearly right.

$$\nu = \nu_0 + \sum_{n=0}^{5}\Delta\nu_n\cdot f_n \tag{6}$$

where ν_0 is the experiment spectral frequency of pure PVME, and n is the subscript. At any step, the total number of waters N_W is certain. It has a relation to f_n:

$$N_W = \sum_{n=0}^{5}100\cdot f_n\cdot n \tag{7}$$

3.4.3. Uneven Distribution of Water on PVME. In the present study, to obtain a better understanding of the beginning steps of the polymer hydration, first we designed two adsorption procedures as Model I and Model II in the examination. Model I is from an ordinary view. Since PVME/H_2O complex is in a homogeneous phase, water molecules should be dispersed individually on the polymer chain, especially in high PVME concentrations. Therefore, in the run of Model I each repeat unit of PVME has the same hydration behavior. For example, in the range of 100~78 wt %, corresponding to zero water molecule/monomer unit (W/M) ~ 1 W/M, each unit prefers to bind with one water by HB. As water increases, till all units have been bound with one water, they begin to bind with the second water, respectively, and then the third, and so on. During the whole hydration process, the hydration degree of each unit contains homogeneous. Model II is a quite different model in which water is not in turn adsorbed on each repeat of PVME chain. As is well known, water molecules are energetically driven to bind together to form water clusters. On this basis, Model II is built up in such way that each repeat unit of PVME prefers to bind once with five water molecules. At first, one unit begins to bind with water. Only after it has bonded with five water molecules can the second unit begin to bind another five, and in turn the rest of the units will bind water in the same way. As a result, all of the units on a PVME chain before the bending point have only two adsorption states: the fifth state and the empty state.

Spectral band shifts of the two models have been calculated using eqs 5−7 as mentioned in the last section and have been compared with the experiment data as shown in Figure 4. It is obvious that the curves of the two models evidently depart from the observed ones. For Model I, there are four bending points that appear in the curves of both $\nu_s(CH_3)$ and $\nu(C-O)$ bands, and they are at 78, 62, 52, and 45 wt %, which corresponding to each repeat unit of PVME has simultaneously bound with one, two, three, and four water molecules, respectively. These bending points divided the curves of Model I into five ranges, which are labeled in turn from high to low concentration as A−E. In the range of A (concentrations higher than 78 wt %), distinct shifts take place for the two bands. It is caused by the unit of PVME interacting with one water. In the range of B and C, spectral bands undergo slight change, which relates either to $\nu_s(CH_3)$ band or to $\nu(C-O)$ band; the spectral influence of two or three water molecules is very close to that of one water molecule. However, large slopes appear again in range D because of the remarkable influence of four water molecules. Then, five water molecules lead to further shift to $\nu_s(CH_3)$ band but does not lead to any effect to $\nu(C-O)$ band as shown in the range of E. For Model II, all the band shifts are caused by five water molecules; therefore, the curves of the two bands are smooth, but they still are not suitable with the experimental data. The departure of these two models suggested that in high concentration, water molecules are not distributed on PVME chain evenly, in other words, the hydration behavior of each repeat unit of PVME is not homogeneous. During the hydration process, there must exist some empty site along the chain where there is no water.

To approach real mechanism of the water adsorption on polymer, we designed another adsorption procedure, as Model

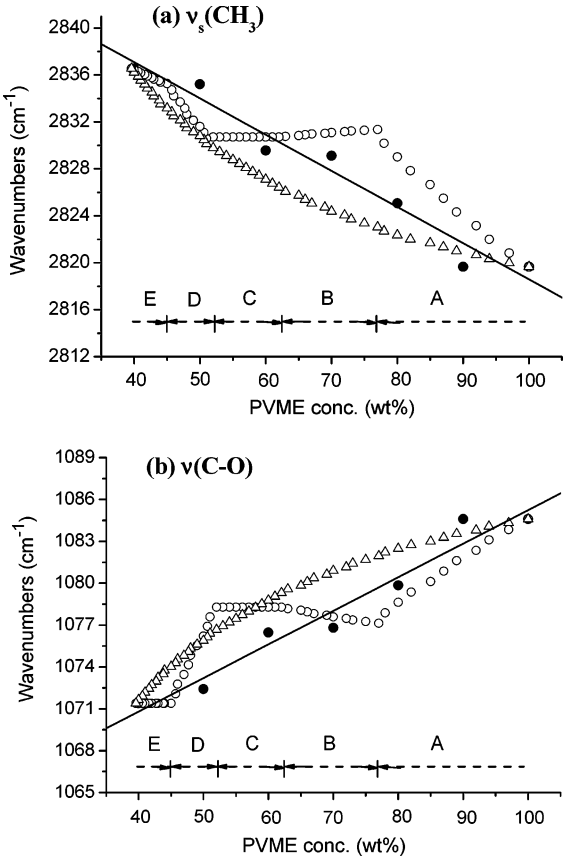

Figure 4. Peak positions of the $\nu_s(CH_3)$ band (a) and ν(C−O) band (b) plotted against polymer concentration. ● is the peak position of experimental data; ○ is the calculated peak position in Model I; △ is the calculated peak position in Model II; the curve is a linear fit of the experimental data.

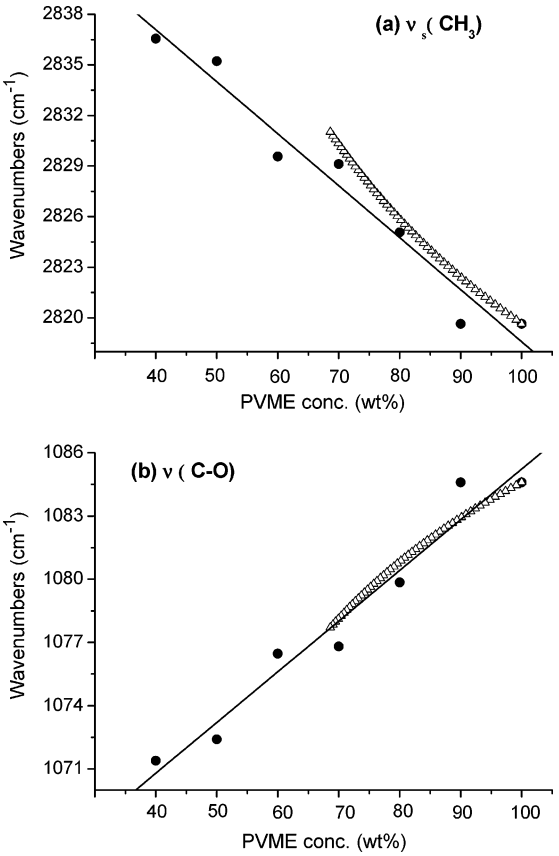

Figure 5. Peak positions of the $\nu_s(CH_3)$ band (a) and ν(C−O) band (b) plotted against polymer concentration. ● is the peak position of experimental data; △ is the calculated peak position in Model III; the curve is a linear fit of the experimental data.

III. In this model, the procedure runs such that the number of water molecules on each repeat unit is alternately to be one or two, such as the unit containing two water molecules always follows the unit containing one water molecule. This model covers a range of 100∼69 wt % (0∼1.5 W/M). As shown in Figure 5, the simulated peak position of Model III is close to the experiment result, especially to the ν(C−O) band. The better fitting of the procedure to the observation shows that Model III is good for this range. During the adsorption process, when it reaches the concentration of 78 wt % (1 W/M), one can still find the empty state, which occupies one-third of all the units. The simulation also shows when the hydration process reaches 69 wt % in an average of 1.5 W/M, all the units of the polymer bind with water or no empty state exists. Even this model describes well the band shift behavior in the range; the adsorption details beyond the range still need further investigation.

4. Conclusion

In the present study, the interaction of water and DME has been investigated by using ab initio quantum mechanics with MP2/6-31+G* for understanding PVME hydration details. In the examination of DME interacting with one to five water molecules, we found two sorts of interactions the HB and the QHB to be specialties. Among the interaction configurations, the interaction energy of HB between water and a DME is larger than the energy between water. We also found that the most stable configuration is with single-HB when the number of water molecules in the interaction ≤3, or with double-HB when the number is beyond 3. The interaction energy of QHB with DME was found remarkably larger than that with methane.

For the influence of the interactions on spectral band shift, the first HB makes a large band shift and the second HB on the same acceptor is able to increase further shift for both the ν(C−O) band (red shift) and the $\nu_s(CH_3)$ band (blue shift). One water molecule binding on the methyl of DME forms single-QHB, which causes a few wavenumber blue shift for ν(C−O) and a several wavenumber red shift for $\nu_s(CH_3)$ and $\nu_{as}(CH_3)$ and a several wavenumber blue shift for the other $\nu_{as}(CH_3)$. When the second or third water binds on the same methyl (forming multiple-QHB), the band shift behaviors for ν(C−O) and $\nu_s(CH_3)$ will turn over.

The present study analyzed different interaction mechanisms between the high concentration area and the low concentration area. All the interaction configurations of DME·nH$_2$O ($n = 1\sim5$) show that in the high concentration area the interaction consists of first HB, second HB, and single-QHB, and in the low concentration area there is no chance to form the second HB but form the double-QHB and the triple-QHB. Therefore, infrared band shift curves of $\nu_s(CH_3)$ and ν(C−O) of PVME hydration show a bending point between the high and the low concentration area because of the different interaction mechanisms.

The beginning steps of PVME hydration were simulated with three models in the present study. Obtained band shift of the two vibration modes as a function of the number of water molecules was adopted. The result shows that even though in thermodynamically equilibrium aqueous solution of PVME the water adsorption on the polymer appears not evenly distributed. When the hydration goes to a state where the concentration is

78 wt % or on average every repeat unit would have a water, the simulation manifests that reasonable distribution is to have one-third the empty state. When one cannot find an empty state on the polymer chain, the hydration process reaches the concentration of 69 wt %, and every repeat unit has 1.5 water molecules on average.

Acknowledgment. This study has been supported by the National Nature Science Foundation, 863 High Technology Project, and the Special Funds for Major State Basic Research Project (G1999064800).

References and Notes

(1) Franks, F. In *Chemistry and Technology of Water-Soluble Polymers*; Finch, C. A., Ed.; Plenum Press: 1983; pp 157−178.
(2) Horne, R. A.; Almeida, J. P.; Day, A. F.; Yu, N.-T. J. *Colloid Interface Sci.* **1971**, *35*, 77.
(3) Molyneyx, P. *Water-soluble Synthetic Polymers: Properties and Behavior*; CRC Press Inc.: Boca Raton, FL, 1983; Vol. I.
(4) Schäfer-Soenen, H.; Moerkerke, R.; Berghmans, H.; Koningsveld, R.; Dušek, K.; Šolc, K. *Macromolecules* **1997**, *30*, 410.
(5) Meeussen, F.; Bauwens, Y.; Moerkerke, R.; Nies, E.; Berghmans, H. *Polymer* **2000**, *41*, 3737.
(6) Zhang, J. M.; Teng, H. X.; Zhou, X. S.; Shen, D. Y. *Polym. Bull.* **2002**, *48*, 277.
(7) Zhang, J. M.; Zhang, G. B.; Wang, J. J.; Lu, Y. L.; Shen, D. Y. *J. Polym. Sci., Part B: Polym. Phys.* **2002**, *40*, 2772.
(8) Zhang, J. M.; Bergé, B.; Meeussen, F.; Nies, E.; Berghmans, H.; Shen, D. Y. *Macromolecules* **2003**, *36* (24), 9145−9153
(9) Maeda, H. *J. Polym. Sci., Part B: Polym. Phys.* **1994**, *32*, 91.
(10) Scheiner, S. *Hydrogen Bonding*; Oxford University Press: New York, 1997; p 11−12.
(11) Nemethy, G.; Scheraga, H. A. *J. Chem. Phys.* **1962**, *36*, 3401.
(12) Frank, H. S.; Evans, M. W. *J. Chem. Phys.* **1945**, *13*, 507.
(13) Tiktopulo, E. I.; Bychkova, V. E.; Ricka, J.; Ptitsyn, O. B. *Macromolecules* **1994**, *27*, 2879.
(14) Liu, K.; Parsons, J. L. *Marcromolecules* **1969**, *2*(5), 529.
(15) Saeki, S.; Kuwahara, N.; Nakata, M.; Kaneko, M. *Polymer* **1976**, *17*, 685.
(16) Meada, Y. *Langmuir* **2001**, *17*, 1737.
(17) Frisch, M. J.; Trucks, G. W.; Schlegel, H. B.; Scuseria, G. E.; Robb, M. A.; Cheeseman, J. R.; Montgomery, J. A., Jr.; Vreven, T.; Kudin, K. N.; Burant, J. C.; Millam, J. M.; Iyengar, S. S.; Tomasi, J.; Barone, V.; Mennucci, B.; Cossi, M.; Scalmani, G.; Rega, N.; Petersson, G. A.; Nakatsuji, H.; Hada, M.; Ehara, M.; Toyota, K.; Fukuda, R.; Hasegawa, J.; Ishida, M.; Nakajima, T.; Honda, Y.; Kitao, O.; Nakai, H.; Klene, M.; Li, X.; Knox, J. E.; Hratchian, H. P.; Cross, J. B.; Adamo, C.; Jaramillo, J.; Gomperts, R.; Stratmann, R. E.; Yazyev, O.; Austin, A. J.; Cammi, R.; Pomelli, C.; Ochterski, J. W.; Ayala, P. Y.; Morokuma, K.; Voth, G. A.; Salvador, P.; Dannenberg, J. J.; Zakrzewski, V. G.; Dapprich, S.; Daniels, A. D.; Strain, M. C.; Farkas, O.; Malick, D. K.; Rabuck, A. D.; Raghavachari, K.; Foresman, J. B.; Ortiz, J. V.; Cui, Q.; Baboul, A. G.; Clifford, S.; Cioslowski, J.; Stefanov, B. B.; Liu, G.; Liashenko, A.; Piskorz, P.; Komaromi, I.; Martin, R. L.; Fox, D. J.; Keith, T.; Al-Laham, M. A.; Peng, C. Y.; Nanayakkara, A.; Challacombe, M.; Gill, P. M. W.; Johnson, B.; Chen, W.; Wong, M. W.; Gonzalez, C.; Pople, J. A. *Gaussian 03*, revision A.6; Gaussian, Inc.: Pittsburgh, PA, 2003.
(18) Garrett, B. C.; Melius, C. F. In *Theoretical and Computational Models for Organic Chemistry*; Formosioho, S. J., et al., Eds.; Kluver Academic: Netherlands, 1991; p 35−54.
(19) Kirtenmacher, H.; Lie, G. C.; Popkie, H.; Clementi, E. *J. Chem. Phys.* **1974**, *61*, 546.
(20) Kim, K. S.; Dupuis, M.; Lie, G. C.; Clementi, C. *Chem. Phys. Lett.* **1986**, *131*, 451.
(21) Honegger, E.; Leutwyler, S. *J. Chem. Phys.* **1988**, *88*, 2582.
(22) Knochenmuss, R.; Leutwyler, S. *J. Chem. Phys.* **1992**, *96*, 5233.
(23) Diercksen, G. H. F.; Kraemer, W. P.; Roos, B. O. *Theor. Chim. Acta* **1975**, *36*, 249.
(24) Yang, X. *Macromolecules* **2001**, *34*, 5037.
(25) Engdahl, A.; Nelander, B. *J. Chem. Soc., Faraday Trans.* **1992**, *88*, 177.
(26) Pugliano, N.; Saykally, R. J. *J. Chem. Phys.* **1992**, *96*, 1832.
(27) Gregory, J. K.; Clay, D. C.; Liu, K.; Brown, M. G.; Saykally, R. J. *Sicence* **1997**, *275*, 814.
(28) Xantheas, S. S.; Dunning, T. H. *J. Chem. Phys.* **1993**, *99*, 8774.
(29) Vergiri, A.; Farantos, S. C. *J. Chem. Phys.* **1993**, *98*, 4059.
(30) Tsai, C. J.; Jordan, K. D. *Chem. Phys. Lett.* **1993**, *213*, 181.
(31) Xantheas, S. S. *J. Chem. Phys.* **1994**, *100*, 7523.
(32) Chalasinki, G.; Szczesniak, M. M.; Scheiner, S. *J. Chem. Phys.* **1991**, *94* (4), 2873.
(33) Pribble, R. N.; Zwier, T. S. *Science* **1994**, *265*, 75.
(34) Mayo, S. L.; Olafson, B. D.; Goddard, W. A.; Skiff, W. M. *J. Am. Chem. Soc.* **1990**, *94*, 8897.
(35) Gu, Y.; Kar, T.; Scheiner, S. *J. Am. Chem. Soc.* **1999**, *121*, 9411.
(36) Lee, H. S.; Wang, Y. K.; Hsu, S. L. *Macromolecules* **1987**, *20*(9), 2089.
(37) Frank, H. S.; Wen, W.-Y. *Faraday Discuss. Chem. Soc.* **1957**, *24*, 133.
(38) Ceccarelli, C.; Jeffery, G. A.; Taylor, R. *J. Mol. Struct.* **1981**, *70*, 255.
(39) Ludwig, R.; Weinhold, F.; Farrar, T. C. *J. Chem. Phys.* **1995**, *102*, 5118.
(40) Chalasinski, G.; Szczesniak, M. M. *J. Chem. Rev.* **1994**, *94*, 1723.
(41) Scheiner, S. *Hydrogen Bonding*; Oxford University Press: New York, 1997; pp 230−231.
(42) Scheiner, S. *Hydrogen Bonding*; Oxford University Press: New York, 1997; pp 298−299.
(43) Hobza, P.; Sandorfy, C. *Can. J. Chem.* **1984**, *62*, 606.
(44) Pross, A.; Radom, L.; Riggs, N. V. *J. Am. Chem. Soc.* **1980**, *102*, 2253.
(45) Barnes, A. J.; Beech, T. R. *Chem. Phys. Lett.* **1983**, *94*. 568.